



A Microstructured Cover Flow Mixer for Hydrothermal Synthesis of ZnO Nanoparticles in Supercritical Water

Kiwamu Sue, Andreas Kölbl, Manfred Kraut & Roland Dittmeyer

To cite this article: Kiwamu Sue, Andreas Kölbl, Manfred Kraut & Roland Dittmeyer (2023) A Microstructured Cover Flow Mixer for Hydrothermal Synthesis of ZnO Nanoparticles in Supercritical Water, Journal of Chemical Engineering of Japan, 56:1, 2197465, DOI: [10.1080/00219592.2023.2197465](https://doi.org/10.1080/00219592.2023.2197465)

To link to this article: <https://doi.org/10.1080/00219592.2023.2197465>



© 2023 The Author(s). Published by Informa UK Limited, trading as Taylor & Francis Group.



Published online: 10 May 2023.



Submit your article to this journal [↗](#)



Article views: 157



View related articles [↗](#)



View Crossmark data [↗](#)

A Microstructured Cover Flow Mixer for Hydrothermal Synthesis of ZnO Nanoparticles in Supercritical Water

Kiwamu Sue^a, Andreas Kölbl^b, Manfred Kraut^b, and Roland Dittmeyer^b

^aResearch Institute for Chemical Process Technology, National Institute of Advanced Industrial Science and Technology (AIST), Tsukuba Central 5, 1-1-1 Higashi, Tsukuba, Ibaraki, 305-8565, Japan^bInstitute for Micro Process Engineering, Karlsruhe Institute of Technology, P.O. Box 3640, Karlsruhe, 76021, Germany

ABSTRACT

A microstructured cover flow mixer equipped with two cyclone structures was used for stable continuous hydrothermal synthesis of ZnO nanoparticles from Zn(NO₃)₂ and NaOH aqueous solutions in supercritical water. The effects of the NaOH/Zn(NO₃)₂ ratio, Zn(NO₃)₂ molality, and flow rate on Zn conversion, crystal structure, particle size, particle morphology, and mixer clogging were examined. The advantages of this mixer were identified by comparing with the results obtained using the same chemical conditions with tee-type, cross-type, and central collision-type mixers.

ARTICLE HISTORY

Received 15 September 2022
Accepted 11 December 2022

KEYWORDS

Cover flow mixer; Cyclone; Clogging prevention; Hydrothermal synthesis; Oxide nanoparticles

1. Introduction

Nanoparticles (NPs) of metal oxides are promising materials for constructing products that are smaller, thinner, lighter, and more functional (Fernández-García and Rodriguez 2008). The performance of NPs strongly depends on particle size, particle size distribution, crystal structure, composition, and crystallinity. Numerous techniques have been proposed for synthesizing NPs on a laboratory scale (Altavilla and Ciliberto 2010) but many of these techniques do not conform to the concepts of green chemistry. In addition, it is difficult to manufacture NPs with desirable properties on an industrial scale, and current techniques require the use of the concentrated base, growth inhibitors, and organic solvents, as well as multistep treatments, long reaction times, and high temperatures above 1000 K.

Continuous hydrothermal synthesis in supercritical water (SCW) is widely recognized as a promising technique for the industrial-scale synthesis of NPs (Adschiri et al. 2011; Erkey and Türk 2021). In this technique, a metal salt aqueous solution is mixed with preheated water in a static mixer using a flow apparatus for high-temperature, high-pressure use and heated rapidly to SCW conditions ($T_C = 647$ K, $P_C = 22.1$ MPa). Metal oxide NPs are continuously produced because the SCW environment supports a high rate of hydrothermal reaction (hydrolysis and dehydration condensation), and the metal oxides are poorly soluble due to the low density and low permittivity of water (Adschiri et al. 2001). However, the utility of this technique as a practical industrial process requires consistent production of NPs

with desirable properties, such as well-controlled particle size, morphology, composition, and structure, as well as the narrow size and composition distributions.

A micromixer is an effective device for the rapid mixing of multiple fluids and promises accurate control of nucleation and growth processes in particle synthesis (Gutierrez et al. 2011). The properties of SCW change drastically with a slight change in temperature or pressure. The rate of hydrothermal reaction and the solubility of metal oxides are also very sensitive to temperature and pressure. Therefore, the time required to heat the metal salt aqueous solution to the reaction temperature strongly affects the characteristics of the synthesized NPs, and the use of a micromixer promotes the synthesis of smaller NPs with a narrow size distribution (Kawasaki et al. 2010). A conventional tee mixer with an inner diameter (i.d.) of <1.0 mm provides good performance at low metal salt molality conditions. In contrast, at high salt molality conditions, there is significant heterogeneous nucleation on the inner wall and clogging of the microchannel of the micromixer. A central collision micromixer (CC) was recently proposed to address these performance issues (Sue et al. 2010). In the CC-type mixer, preheated water is fed equally from four directions at right angles into a straight channel (0.3 mm i.d.). The metal salt aqueous solution is fed from the straight channel and mixed with the preheated water. This channel structure reduces the contact of the metal salt aqueous solution with the inner wall just after the mixing point and works well for homogeneous nucleation in reaction systems with a very high rate of hydrothermal reaction without base, such as Fe₂O₃, ZrO₂, TiO₂, and spinel ferrites syntheses (Sue et al. 2006; Sue, Aoki,

CONTACT Kiwamu Sue  k.sue@aist.go.jp; Manfred Kraut  manfred.kraut@kit.edu

© 2023 The Author(s). Published by Informa UK Limited, trading as Taylor & Francis Group. This is an Open Access article distributed under the terms of the Creative Commons Attribution-NonCommercial License (<http://creativecommons.org/licenses/by-nc/4.0/>), which permits unrestricted non-commercial use, distribution, and reproduction in any medium, provided the original work is properly cited. The terms on which this article has been published allow the posting of the Accepted Manuscript in a repository by the author(s) or with their consent.

et al. 2011; Sue, Kawasaki, et al. 2011). Therefore, novel mixers for relative low reaction rate systems may be the key to achieving homogeneous nucleation and preventing clogging both near the mixing point and in the reaction zone after mixing.

A microstructured cover flow mixer was recently developed at the Institute for Micro Process Engineering, Karlsruhe Institute of Technology (Kraut et al. to be published). The mixer is equipped with two cyclone structures (Figure 1). Each cyclone structure has two inlets. The first cyclone structure is used for the fast mixing of two solutions to produce particles or precursors. The second cyclone structure is arranged to supply additional liquid to surround the mixture stream from the first cyclone and to heat the mixture stream during continuous hydrothermal synthesis under SCW conditions for producing metal oxide NPs. This structure prevents contact of the mixture stream with the inner wall of the mixer.

The contribution of this study is to describe the hydrothermal synthesis of ZnO NPs in SCW using this microstructured cover flow mixer. ZnO synthesis from $\text{Zn}(\text{NO}_3)_2$ and NaOH was selected as a typical system that the use of bases is indispensable because the hydrothermal reaction rate of ZnO synthesis without base is low (Sato et al. 2008). The effects of $\text{Zn}(\text{NO}_3)_2$ molality and flow rate on particle size, particle size distribution, and pressure fluctuations during the synthesis were studied. The advantages of the cover flow mixer are discussed by comparison with results obtained using conventional tee-type, cross-type, and CC-type mixers.

2. Experimental

2.1 Materials

$\text{Zn}(\text{NO}_3)_2$ aqueous solutions were prepared by dissolving appropriate amounts of $\text{Zn}(\text{NO}_3)_2 \cdot 6\text{H}_2\text{O}$ (purity 99.9%; Wako Pure Chemical Industries, Ltd.) in deionized water. NaOH aqueous solutions were prepared by dissolving appropriate amounts of NaOH (purity 98.3%; Wako) in deionized water under an N_2 atmosphere. The molality of $\text{Zn}(\text{NO}_3)_2$ was set to 0.05, 0.10, and 0.20 mol/kg. The molality of NaOH was set to 0.10, 0.20, and 0.40 mol/kg to keep constant the molar ratio of NaOH to NO_3^- ($R=1.00$). In addition, the NaOH molality for the 0.20 mol/kg $\text{Zn}(\text{NO}_3)_2$ condition was varied from 0.20 to 0.50 mol/kg ($R=0.50-1.25$) to determine the appropriate NaOH molality for producing ZnO NPs.

2.2 Apparatus and procedure

A schematic diagram of the experimental apparatus for continuous hydrothermal synthesis is shown in Figure 2, and details of the microstructured cover flow mixer are shown in Figures 1 and 3. The $\text{Zn}(\text{NO}_3)_2$ and NaOH aqueous solutions were fed into the first cyclone (Figures 1(a,b)) in the cover flow mixer and then mixed using cyclone flow. Water was heated, divided into two channels (Figure 3(a)), then fed into the second cyclone stage (Figures 1(a,c)) using cyclone flow. The solution of $\text{Zn}(\text{NO}_3)_2$ and NaOH was surrounded by the preheated water, and the solution was

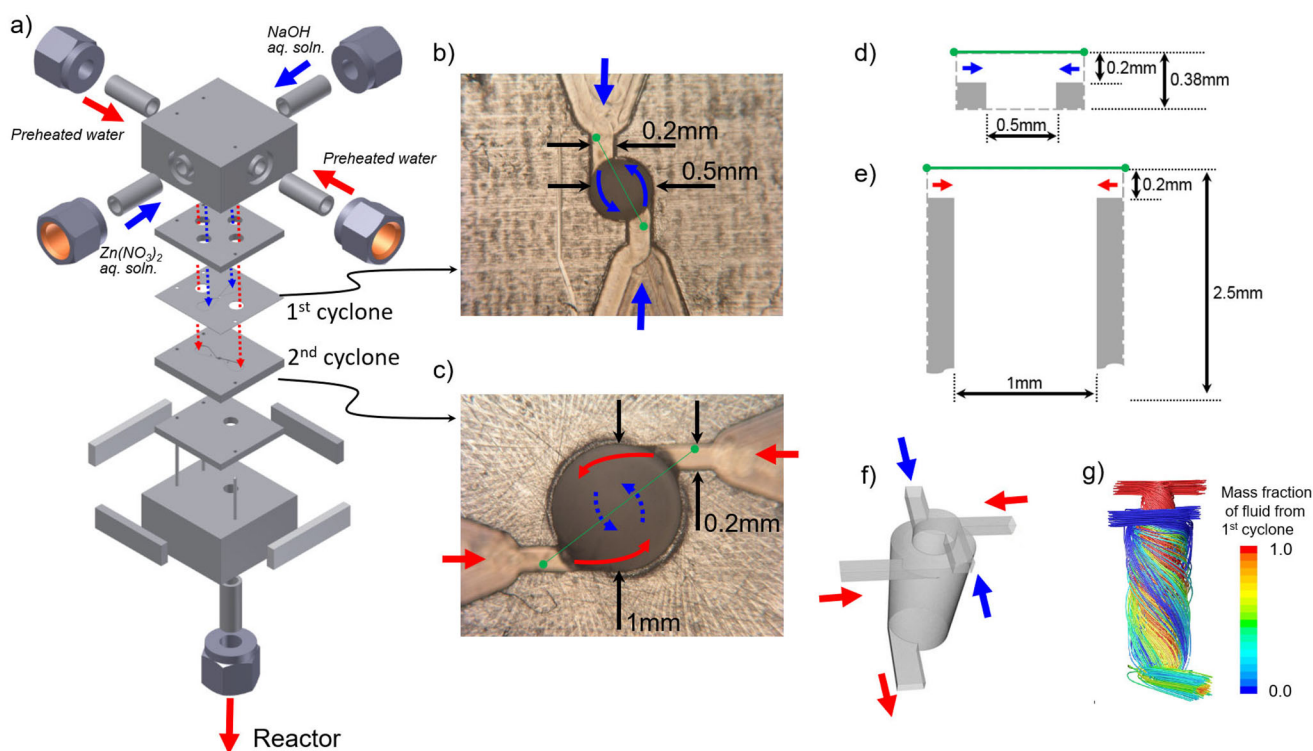


Figure 1. Detailed structure of the microstructured cover flow mixer for ZnO nanoparticles synthesis. (a) Overall structure. (b) Top view of the first cyclone plate. (c) Top view of the second cyclone plate. (d) Cross-sectional view along the green line in (b) of the first cyclone mixer. (e) Cross-sectional view along the green line in (c) of the second cyclone. (f) Channel structure. (g) Streamline image.

heated to the reaction temperature as it mixed with the preheated water. During heating, the preheated water acts as a cover flow for preventing clogging and helps promote homogeneous nucleation. A tubular reactor (1.7 mm i.d., 550 mm long) was connected at the exit of the cover flow mixer. The reaction was stopped by using an air- and water-cooled heat exchanger. NPs were separated from the slurry by using an inline filter with a pore size of 2.0 μm . The NPs recovered from the inline filter were washed with pure water and then dried at 333 K in an electric oven for 24 h. The temperature of the preheated water was directly monitored using a thermocouple and was maintained at around 703 K.

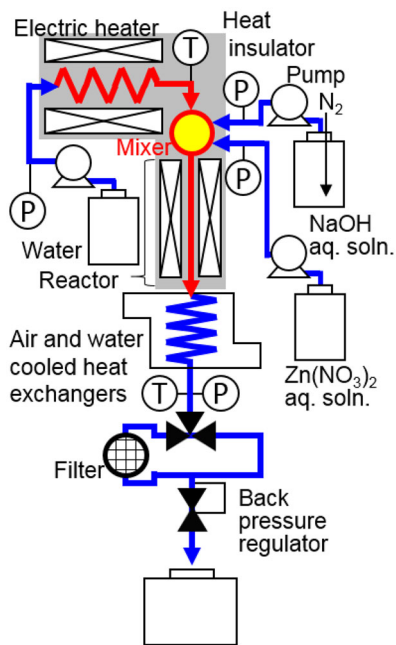


Figure 2. Schematic diagram of the experimental apparatus for continuous hydrothermal synthesis.

Under these conditions, the temperature of the mixed fluid after the second cyclone was estimated to be 673 K based on an enthalpy balance calculation using the flow rates and enthalpies of the preheated water, $\text{Zn}(\text{NO}_3)_2$ solution, and NaOH solution. The temperature of the reactor was controlled at 673 ± 0.2 K using an electric heater and a thermocouple fastened to the reactor tubing. The reaction pressure in the apparatus was controlled at 30 ± 0.2 MPa using a back pressure regulator. Typical flow rates of water and the $\text{Zn}(\text{NO}_3)_2$ and NaOH aqueous solutions were 60.0, 7.5, and 7.5 g/min, respectively. Three total flow rate conditions of 25, 50, and 75 g/min at the same flow rate ratio were examined to evaluate the performance of the cover flow mixer. Depending on the flow rate, the mean residence time was calculated to be 0.36, 0.54, and 1.07 s based on the total flow rate, reactor volume, and water density. For comparison, five conventional mixers (three tee mixers (0.3, 1.3, and 2.3 mm i.d.), a cross mixer (1.3 mm i.d.), and a central collision micromixer (0.3 mm i.d.) were also used, as shown in Figures 3(b–f). During some experiments, the measured pressure increased due to a decrease in channel cross-sectional area caused by the precipitation of the products on the inner walls of the mixers and the reactor tube. To evaluate this behavior, clogging time was defined as the time from the start of feeding the reaction solution into the reactor to when the pressure first increased above 30 MPa.

2.3 Analyses

Crystal structures were analyzed by X-ray powder diffraction (XRD, MiniFlex II, Rigaku) using $\text{CuK}\alpha$ radiation. Crystallite size was calculated based on the full width at half-maximum of the ZnO (100) and (002) peaks using the Scherrer equation. The value is shown as a complementary information for particle size from TEM observation because this evaluation is not suitable for a detail discussion of the

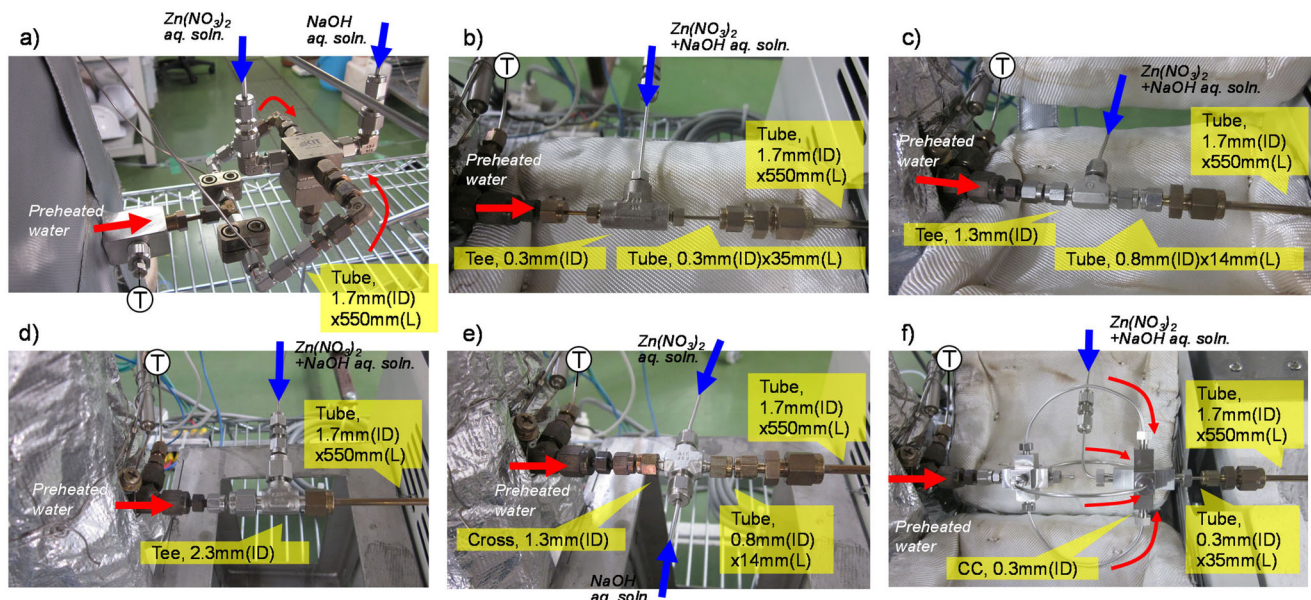


Figure 3. Views of the mixers. (a) Cover flow mixer. (b) Tee mixer (0.3 mm i.d.). (c) Tee mixer (1.3 mm i.d.). (d) Tee mixer (2.3 mm i.d.). (e) Cross mixer (1.3 mm i.d.). (f) Central collision micromixer (0.3 mm i.d.).

crystals with a broad size distribution. Observations were performed by transmission electron microscopy (TEM, JEM-2100, JEOL). The average particle size (APS) and standard deviation (SD) were determined by measuring the sizes of 500 particles on several TEM images. The molality of the Zn ionic species remaining in the recovered aqueous solution was measured by microwave plasma-atomic emission spectrometry (4200, Agilent) to obtain the conversion of dissolved ionic species of Zn to solid products. The recovered solution was filtrated with a membrane filter with a pore size of 25 nm before the measurement and a significant amount of product was not observed. APS was also evaluated from ZnO density (5.6 g/cm^3) and surface area measured by BET surface area analysis (NOVA 3200, Quantachrome) and assuming spherical particles.

3. Results and discussion

3.1 Effects of NaOH molality

The effects of NaOH molality on the hydrothermal synthesis of ZnO NPs were examined at a total flow rate of 75 g/min and a $\text{Zn}(\text{NO}_3)_2$ molality of 0.20 mol/kg. XRD patterns of the products are shown in Figure 4. All diffraction peaks of the products synthesized in this work could be indexed as the wurtzite phase of ZnO (JCPDS card no. 36-1451). Zn conversion dramatically increased with increasing NaOH molality, from 55% at $R=0.5$ to 100% at $R=1.0$, as shown in Table 1; further increase in the NaOH molality showed no significant difference. Typical TEM images at given R values are shown in Figure 5 and NPs with different aspect ratios were observed. APSs calculated using the long and short axis lengths of each particle (APS-L and APS-S, respectively) are shown in Table 1 and Figure 6(a). APS-L remarkably decreased with increasing NaOH molality, from 157 nm at $R=0.5$ to 30 nm at $R=1.0$, and then increased to 71 nm at $R=1.25$. APS-S slightly decreased with increasing NaOH molality, from 45 nm at $R=0.5$ to 17 nm at $R=1.0$, and then increased to 27 nm at $R=1.25$. The crystallite size obtained from the (100) and (002) planes and APS evaluated from BET surface area are shown in Figures 6(b,c),

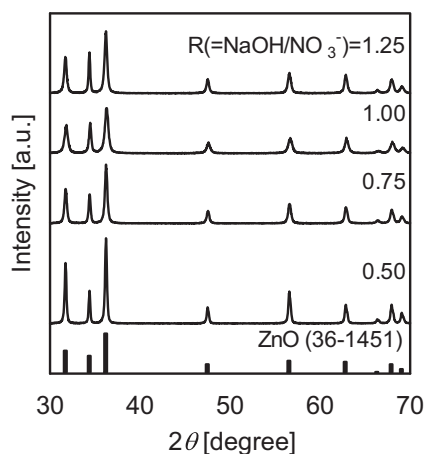


Figure 4. XRD patterns of the products were synthesized using the cover flow mixer at a flow rate of 75 g/min and a $\text{Zn}(\text{NO}_3)_2$ molality of 0.20.

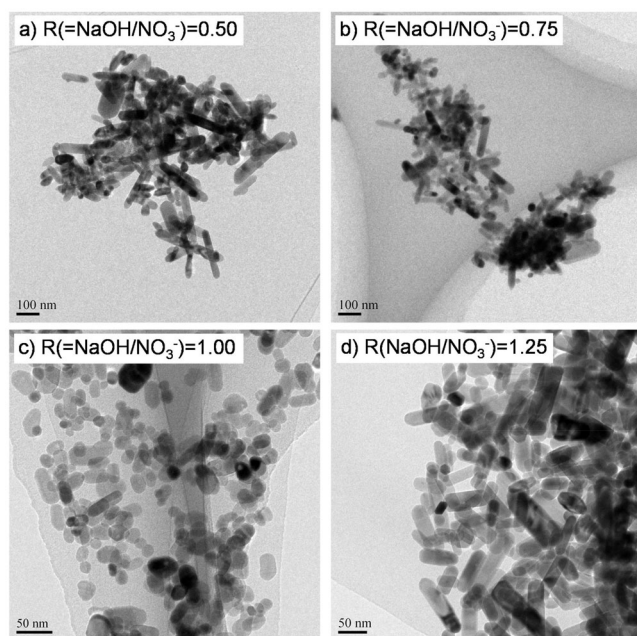
respectively, and all showed a similar trend with increasing NaOH molality. The error bars in Figures 6(a,b) mean standard deviation (SD) for the estimation of APS and the crystallite size, respectively. The changes in growth direction corresponded to the crystallite anisotropy of ZnO, with the relative growth orientation along the c -axis, that is, the (002) plane, owing to polarity in the crystal system (Demoisson et al. 2014; Liu and Zeng 2003). ZnO solubility decreases as conditions are changed from acidic to neutral, and then increases under basic conditions even under high-temperature, high-pressure conditions (Bénézech et al. 2002). In addition, the Zn^{2+} species in solution changes from ZnOH^+ under acidic conditions to $\text{Zn}(\text{OH})_2^0$ under neutral conditions, and further to $\text{Zn}(\text{OH})_3^-$ and $\text{Zn}(\text{OH})_4^{2-}$ under basic conditions. Given these equilibria, the experimental results can be explained as follows. Under neutral conditions ($R=1.00$), concentration of neutral species ($\text{Zn}(\text{OH})_2^0$) is very low and the coexistence does not strongly affect nucleation and growth. Very low ZnO solubility results in the formation of smaller ZnO NPs with a low aspect ratio and also in high Zn conversion due to the high nucleation rate. Under acidic conditions ($R=0.50$ and 0.75), high ZnO solubility and the coexistence of cationic species (Zn^{2+} , ZnOH^+) cause a low nucleation rate and additional growth processes along the c -axis. Growth occurs mainly on negatively charged oxygen-terminated (000-1) planes, and results in the formation of larger ZnO NPs with high aspect ratio and also in low Zn conversion. Under basic conditions ($R=1.25$), ZnO solubility is likely not very high given the high Zn conversion; therefore, most Zn species immediately nucleate, and the coexistence of low-concentration anionic species ($\text{Zn}(\text{OH})_3^-$ and $\text{Zn}(\text{OH})_4^{2-}$) causes additional nucleation and slight growth along the c -axis, mainly on positively charged zinc-terminated (0001) planes. Orita et al. (2019) carefully examined the anisotropic growth of ZnO nanoparticles during supercritical hydrothermal continuous synthesis by time-resolved experiments, analyzed the growth rate based on a kinetic analysis and chemical equilibrium calculations, and reported a similar trend that the growth rate increased at acidic and basic condition.

3.2 Effects of $\text{Zn}(\text{NO}_3)_2$ molality and flow rate

The effects of $\text{Zn}(\text{NO}_3)_2$ molality and flow rate on the hydrothermal synthesis of ZnO NPs were examined at $R=1.00$. The Zn conversion was above 99% under all conditions studied. The APSs are shown in Table 1 and Figure 7(a), the crystallite sizes are shown in Figure 7(b), and the particle size distributions of the products are shown in Figure 8. Similar trends were observed for APS and crystallite size: the long-axis size decreased with increasing $\text{Zn}(\text{NO}_3)_2$ molality and flow rate. As shown in Table 1 and Figure 9, no clogging occurred at a total flow rate of 75 g/min and ZnO NPs were stably produced. However, clogging increased remarkably with decreasing $\text{Zn}(\text{NO}_3)_2$ molality and flow rate. We offer the following explanation for these results. At a high flow rate, $\text{Zn}(\text{NO}_3)_2$ and NaOH aqueous solutions are instantly mixed in the first cyclone

Table 1. Summary of experiments on continuous hydrothermal synthesis of ZnO nanoparticles.

Mixer type	Zn(NO ₃) ₂ (mol/kg)	R(=NaOH/NO ₃ ⁻) (-)	Flow rate (g/min)	Clogging time (min)	APS-L/SD (nm)	APS-S/SD (nm)	Zn conversion (%)
Cover flow	0.20	0.50	75	1	157/147	45/22	55
	0.20	0.75		-	110/134	38/23	78
	0.20	1.25		-	71/38	27/7	100
	0.20	1.00	75	-	30/20	17/6	100
	0.10	-		-	31/21	18/6	100
	0.05	-		-	37/26	19/8	100
	0.20	1.00	50	-	43/30	21/7	100
	0.10	-		-	48/40	22/10	100
	0.05	-		20	49/38	22/9	100
	0.20	1.00	25	10	48/34	22/9	100
	0.10	-		10	53/50	22/10	100
	0.05	-		6	61/50	25/10	99
	Tee, 0.3 mm ID	0.20	1.00	75	2	64/38	29/10
Tee, 1.3 mm ID				1	51/30	35/14	100
Tee, 2.3 mm ID				-	70/55	38/17	100
Cross, 1.3 mm ID				15	40/28	19/8	100
Central collision				2	65/58	31/16	100

**Figure 5.** TEM images of the products were synthesized using the cover flow mixer at a flow rate of 75 g/min and a Zn(NO₃)₂ molality of 0.20.

and the nucleation precursor, Zn(OH)₂, is immediately produced. The mixture is mixed with preheated water after the second cyclone stage, heated to the reaction temperature by the surrounding preheated water, and finally converted to a slurry containing small ZnO NPs with a narrow size distribution. At a low flow rate, the Zn(NO₃)₂ and NaOH aqueous solutions are fed into the second cyclone before they are mixed well enough to produce a uniform precursor. This non-uniform mixture is slowly mixed with preheated water in the second cyclone and gradually converted into a slurry that contains large ZnO NPs with a wide size distribution. During mixing after the second cyclone, the molality distribution of Zn(NO₃)₂ and NaOH forms high and low *R* reaction fields and causes undesirable heterogeneous nucleation, undesirable growth, and clogging, as described in Section 1. Further, if the reaction proceeds after the completion of mixing (i.e., after reaching the reaction temperature), the

reactant solution contacts the inner wall of the channel, leading to heterogeneous nucleation, undesirable growth, and clogging. Previous studies of continuous hydrothermal synthesis shed light on the effects of molality of metal salts (Cote et al. 2003; Gruar et al. 2013; Hao and Teja 2003; Sue et al. 2004, 2010; Sue, Aoki, et al. 2011) by showing that the APS of metal oxides increases with increasing molality of metal salts. This trend is likely due to particle growth and aggregation in high ionic strength media (Bian et al. 2011) and due to heterogeneous nucleation on the inner walls of the mixer and the reactor. In the present study, the opposite trend was observed: APS gradually decreased with an increase in Zn(NO₃)₂ molality, even under low flow rate conditions. In SCW, strong electrolytes, such as NaCl do not dissociate and behave like weak electrolytes due to the very low dielectric constant of SCW (Ho et al. 2000). This reduces the effect of ionic strength and affects ZnO solubility under different molality conditions. If ZnO solubility is almost constant, then the degree of supersaturation increases with increasing Zn(NO₃)₂ molality, and smaller NPs are produced. Taken together, these results suggest that an increase in supersaturation and prevention of heterogeneous nucleation in the cover flow mixer are major factors in decreasing APS with an increase in Zn(NO₃)₂ molality.

3.3 Comparison with conventional mixers

The cover flow mixer was compared with five conventional mixers [three tee mixers (0.3, 1.3, and 2.3 mm i.d.), a cross mixer (1.3 mm i.d.), and a central collision micromixer (0.3 mm i.d.)] as shown in Figure 3 at a Zn(NO₃)₂ molality of 0.20, *R*=1.00, and a total flow rate of 75 g/min. For experiments conducted using the tee mixers and the central collision mixer, the Zn(NO₃)₂ and NaOH aqueous solutions were first mixed using the 0.5 mm i.d. tee mixer to form the Zn(OH)₂ precursor. This mixture was then supplied to the tee and central collision mixers for heating, as shown in Figure 3. The APS and standard deviation of the products, and the clogging time, are summarized in Table 1, and the particle size distributions are shown in Figure 8. The use of

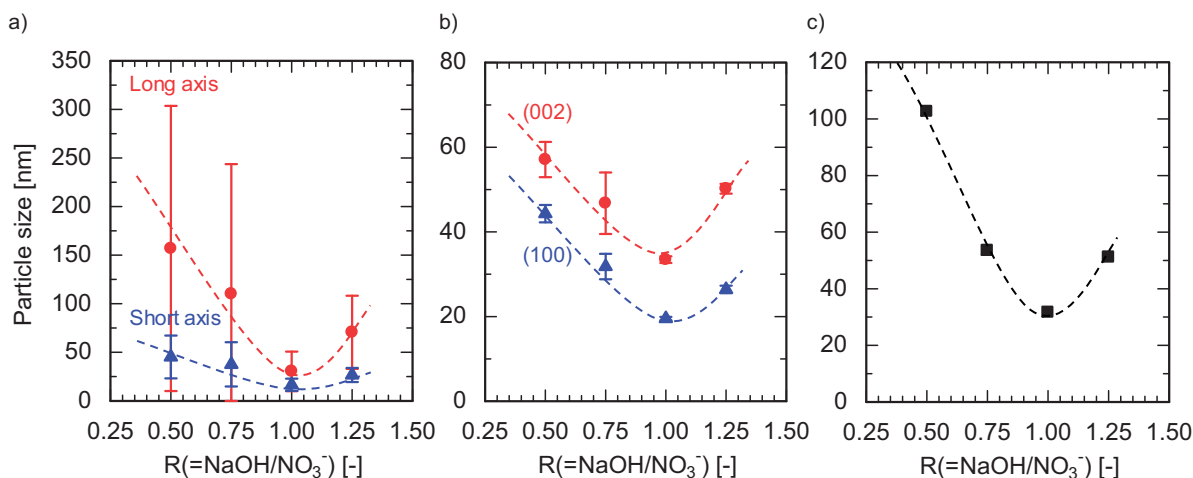


Figure 6. Variation in APS with $R(=\text{NaOH}/\text{NO}_3^-)$ evaluated by (a) TEM, (b) XRD, and (c) BET surface area analysis. The dashed lines illustrate the trend.

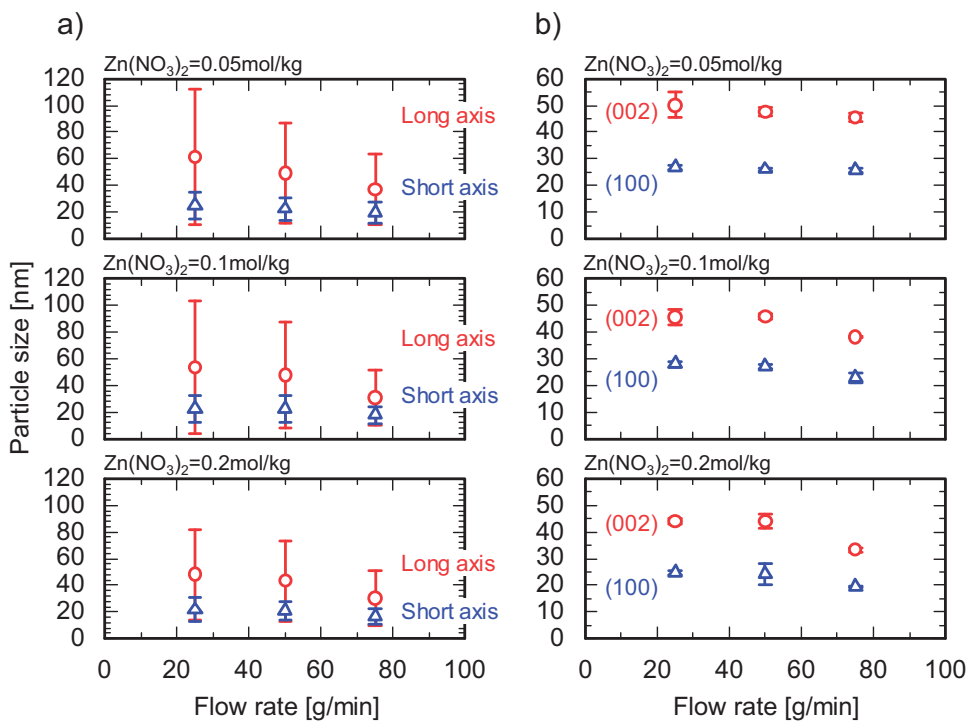


Figure 7. Variation in APS with flow rate at different $\text{Zn}(\text{NO}_3)_2$ molarities evaluated by (a) TEM, and (b) XRD analyses.

the tee mixers provided NPs with remarkably decreased long-axis APS, from 70 to 51 nm, and the particle size distribution slightly narrowed with a decrease in i.d. from 2.3 to 1.3 mm. However, a further decrease in i.d. to 0.3 mm provided NPs with an increased long-axis APS (64 nm) and a wide particle size distribution, despite the increased mixing and heating rates. Heterogeneous nucleation and subsequent growth in the narrow microchannel after the mixing point likely occurred due to the increase in the surface area to volume ratio. Using the central collision mixer provided NPs with an APS of around 64–65 nm for the long axis and 29–31 nm for the short axis, similar to the APS obtained with the tee mixer (0.3 mm i.d.). It is notable that the products obtained using the central collision mixer included large particles of between 50 and 250 nm, as shown in Figure 8,

and the pressure in the central collision mixer system sharply increased compared with that in the tee mixer systems, as shown in Figure 9. The heating time (mixing time) in the central collision mixer was about 6-fold that in a tee mixer (Sue et al. 2010). If nucleation is not complete during this period, there is a very large effect due to heterogeneous nucleation and growth on the inner surface of the mixer and of the first tube reactor (0.3 mm i.d.) in the central collision mixer. In the cross mixer (1.3 mm i.d.), small NPs with a narrow size distribution were produced, and the clogging time was remarkably longer than that of the tee mixer with the same diameter (1.3 mm i.d.). In the tee mixer, the $\text{Zn}(\text{NO}_3)_2$ aqueous solution was mixed with preheated water after mixing with NaOH, so the $\text{Zn}(\text{OH})_2$ precursor was formed before heating and nucleation (homogeneous and

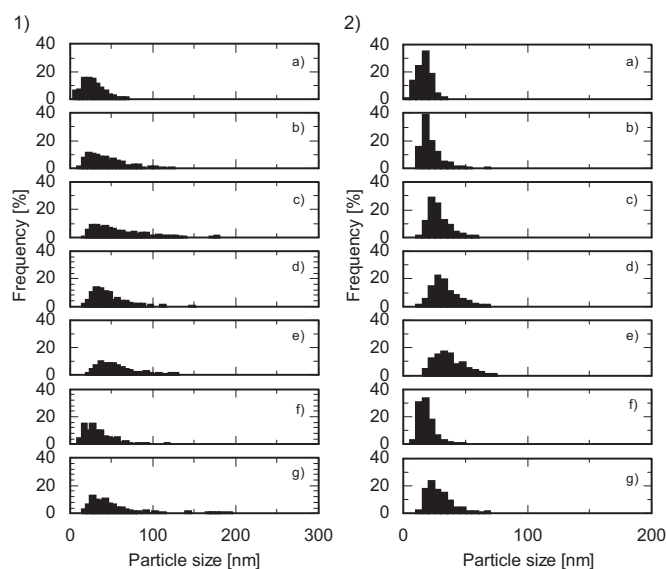


Figure 8. Particle size distributions (1) long axis, (2) short axis of the products synthesized using a $\text{Zn}(\text{NO}_3)_2$ molality of 0.20 in a (a) cover flow micromixer (75 g/min), (b) cover flow mixer (25 g/min), (c) tee mixer (0.3 mm i.d., 75 g/min), (d) tee mixer (1.3 mm i.d., 75 g/min), (e) tee mixer (2.3 mm i.d., 75 g/min), (f) cross mixer (1.3 mm i.d., 75 g/min), and (g) central collision micromixer (0.3 mm i.d., 75 g/min).

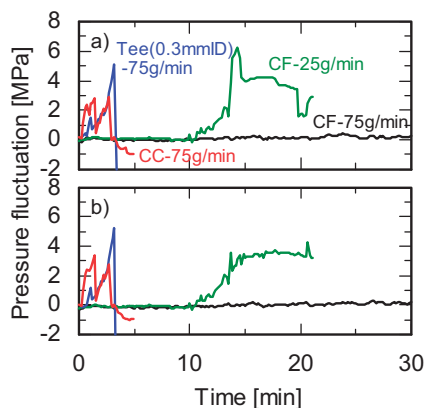


Figure 9. Variation of pressure fluctuation in the (a) water and (b) $\text{Zn}(\text{NO}_3)_2$ channels with time during the experiment using different mixers.

heterogeneous) starts and probably finishes in the first tube reactor (0.8 mm i.d.) during mixing with preheated water, as shown in Figure 3(e). In contrast, in the cross mixer, $\text{Zn}(\text{NO}_3)_2$ aqueous solution was mixed with NaOH in parallel with mixing with preheated water. Consequently, the formation of the $\text{Zn}(\text{OH})_2$ precursor and further nucleation of ZnO were relatively slow in the cross mixer compared with the tee mixer. The $\text{Zn}(\text{OH})_2$ precursor forms in the first tube reactor (0.8 mm i.d.) and nucleation finishes in the second tube reactor, as shown in Figure 3(f). A higher inner surface area to volume ratio in the tube causes heterogeneous nucleation (clogging) and the formation of larger particles. Therefore, the use of the cross mixer resulted in long clogging times and the formation of small NPs. Compared with these conventional mixers, the cover flow mixer holds promise for the stable production of very small NPs with narrow size distributions.

4. Conclusion

Continuous hydrothermal synthesis of ZnO nanoparticles in SCW at 673 K and 30 MPa was performed using a microstructured cover flow mixer equipped with two cyclone structures. ZnO NPs with an APS of 30 nm and 100% Zn conversion were stably produced without clogging the mixer at a high flow rate of 75 g/min under neutral solution conditions with low ZnO solubility (i.e., $\text{NaOH}/\text{Zn}(\text{NO}_3)_2$ molar ratio = 2.0). Using the same conditions, previously reported tee-type, cross-type, and central collision-type mixers became clogged, and/or large NPs with a relatively broad size distribution were formed. The results demonstrated that the cover flow mixer is advantageous for preventing clogging (i.e., promoting homogeneous nucleation) and for producing small NPs with a narrow size distribution.

Acknowledgments

TEM observations were performed using facilities at the Institute for Solid State Physics (ISSP), the University of Tokyo. The authors greatly appreciate the efforts of Dr. Daisuke Nishio-Hamane (ISSP) for the TEM observation.

Funding

This work was partially supported by JSPS KAKENHI Grant Number JP23686113.

References

- Adschiri T, Hakuta Y, Sue K, Arai K. 2001. Hydrothermal synthesis of metal oxide nanoparticles at supercritical conditions. *J Nanopart Res.* 3:227–235. doi: [10.1023/A:1017541705569](https://doi.org/10.1023/A:1017541705569)
- Adschiri T, Lee Y-W, Goto M, Takami S. 2011. Green materials synthesis with supercritical water. *Green Chem.* 13:1380–1390. doi: [10.1039/c1gc15158d](https://doi.org/10.1039/c1gc15158d)
- Altavilla C, Ciliberto E. 2010. *Inorganic nanoparticles: synthesis, applications, and perspectives (nanomaterials and their applications)*. Boca Raton (FL); London; New York (NY): CRC Press.
- Bénéthet P, Palmer DA, Wesolowski DJ, Xiao C. 2002. New measurements of the solubility of zinc oxide from 150 to 350 °C. *J Sol Chem.* 31:947–973. doi: [10.1023/A:1021866025627](https://doi.org/10.1023/A:1021866025627)
- Bian S-W, Mudunkotuwa IA, Rupasinghe T, Grassian VH. 2011. Aggregation and dissolution of 4 nm ZnO nanoparticles in aqueous environments: influence of pH, ionic strength, size, and adsorption of humic acid. *Langmuir.* 27:6059–6068. doi: [10.1021/la200570n](https://doi.org/10.1021/la200570n)
- Cote LJ, Teja AS, Wilkinson AP, Zhang ZJ. 2003. Continuous hydrothermal synthesis of CoFe_2O_4 nanoparticles. *Fluid Phase Equilib.* 210:307–317. doi: [10.1016/S0378-3812\(03\)00168-7](https://doi.org/10.1016/S0378-3812(03)00168-7)
- Demoisson F, Piolet R, Ariane M, Leybros A, Bernard F. 2014. Influence of the pH on the ZnO nanoparticle growth in supercritical water: experimental and simulation approaches. *J Supercrit Fluids.* 95:75–83. doi: [10.1016/j.supflu.2014.08.007](https://doi.org/10.1016/j.supflu.2014.08.007)
- Erkey C, Türk M. 2021. *Synthesis of nanostructured materials in near and/or supercritical fluids: methods, fundamentals and modeling*. San Diego (CA): Elsevier.
- Fernández-García M, Rodríguez JA. 2008. Metal oxide nanoparticles. In: Lukehart CM, Scott RA, editors. *Nanomaterials: inorganic and bioinorganic perspectives*. New York (NY): John Wiley & Sons. p. 453–474.
- Gruar RI, Tighe CJ, Darr JA. 2013. Scaling-up a confined jet reactor for the continuous hydrothermal manufacture of nanomaterials. *Ind Eng Chem Res.* 52:5270–5281. doi: [10.1021/ie302567d](https://doi.org/10.1021/ie302567d)

- Gutierrez L, Gomez L, Irusta S, Arruebo M, Santamaria J. 2011. Comparative study of the synthesis of silica nanoparticles in micro-mixer–microreactor and batch reactor systems. *Chem Eng J*. 171: 674–683. doi: [10.1016/j.cej.2011.05.019](https://doi.org/10.1016/j.cej.2011.05.019)
- Hao Y, Teja AS. 2003. Continuous hydrothermal crystallization of Fe₂O₃ and Co₃O₄ nanoparticles. *J Mater Res*. 18:415–422. doi: [10.1557/JMR.2003.0053](https://doi.org/10.1557/JMR.2003.0053)
- Ho PC, Bianchi H, Palmer DA, Wood RH. 2000. Conductivity of dilute aqueous electrolyte solutions at high temperatures and pressures using a flow cell. *J Sol Chem*. 29:217–235. doi: [10.1023/A:1005146332605](https://doi.org/10.1023/A:1005146332605)
- Kawasaki S-I, Sue K, Ookawara R, Wakashima Y, Suzuki A, Hakuta Y, Arai K. 2010. Engineering study of continuous supercritical hydrothermal method using a T-shaped mixer: experimental synthesis of NiO nanoparticles and CFD simulation. *J Supercrit Fluids*. 54:96–102. doi: [10.1016/j.supflu.2010.03.001](https://doi.org/10.1016/j.supflu.2010.03.001)
- Kraut M, Köbl A, Forconi M, Wenka A, Sue K, Dittmeyer R. to be published.
- Liu B, Zeng HC. 2003. Hydrothermal synthesis of ZnO nanorods in the diameter regime of 50 nm. *J Am Chem Soc*. 125:4430–4431. doi: [10.1021/ja0299452](https://doi.org/10.1021/ja0299452)
- Orita Y, Akizuki M, Oshima Y. 2019. Kinetic analysis of zinc oxide anisotropic growth in supercritical water. *J Supercrit Fluids*. 154: 104609. doi: [10.1016/j.supflu.2019.104609](https://doi.org/10.1016/j.supflu.2019.104609)
- Sato T, Sue K, Suzuki W, Suzuki M, Matsui K, Hakuta Y, Hayashi H, Arai K, Kawasaki S-I, Kawai-Nakamura A, et al. 2008. Rapid and continuous production of ferrite nanoparticles by hydrothermal synthesis at 673 K and 30 MPa. *Ind Eng Chem Res*. 47:1855–1860. doi: [10.1021/ie071168x](https://doi.org/10.1021/ie071168x)
- Sue K, Aoki M, Sato T, Nishio-Hamane D, Kawasaki S-I, Hakuta Y, Takebayashi Y, Yoda S, Furuya T, Sato T, et al. 2011. Continuous hydrothermal synthesis of nickel ferrite nanoparticles using a central collision-type micromixer: effects of temperature, residence time, metal salt molality, and NaOH addition on conversion, particle size, and crystal phase. *Ind Eng Chem Res*. 50:9625–9631. doi: [10.1021/ie200036m](https://doi.org/10.1021/ie200036m)
- Sue K, Kawasaki S-i, Suzuki M, Hakuta Y, Hayashi H, Arai K, Takebayashi Y, Yoda S, Furuya T. 2011. Continuous hydrothermal synthesis of Fe₂O₃, NiO, and CuO nanoparticles by superrapid heating using a T-type micro mixer at 673 K and 30 MPa. *Chem Eng J*. 166:947–953. doi: [10.1016/j.cej.2010.11.080](https://doi.org/10.1016/j.cej.2010.11.080)
- Sue K, Kimura K, Murata K, Arai K. 2004. Effect of cations and anions on properties of zinc oxide particles synthesized in supercritical water. *J Supercrit Fluids*. 30:325–331. doi: [10.1016/j.supflu.2003.09.009](https://doi.org/10.1016/j.supflu.2003.09.009)
- Sue K, Sato T, Kawasaki S, Takebayashi Y, Yoda S, Furuya T, Hiaki T. 2010. Continuous hydrothermal synthesis of Fe₂O₃ nanoparticles using a central collision-type micromixer for rapid and homogeneous nucleation at 673 K and 30 MPa. *Ind Eng Chem Res*. 49: 8841–8846. doi: [10.1021/ie1008597](https://doi.org/10.1021/ie1008597)
- Sue K, Suzuki M, Arai K, Ohashi T, Ura H, Matsui K, Hakuta Y, Hayashi H, Watanabe M, Hiaki T. 2006. Size-controlled synthesis of metal oxide nanoparticles with a flow-through supercritical water method. *Green Chem*. 6:634–638.